CHEMISTRY
A EUROPEAN JOURNAL

High Surface Area, Mesoporous, Glassy Alumina with a Controllable Pore Size by Nanocasting from Carbon Aerogels

Wen-Cui Li, An-Hui Lu, Wolfgang Schmidt, and Ferdi Schüth*[a]

Abstract: A strategy to synthesize amorphous, mesoporous alumina by nanocasting has been developed, involving carbon aerogel as a hard template and aluminum nitrate solution as an alumina precursor. The alumina generated exhibits small, transparent granules with a 3–6 mm diameter and has inherited the three-dimensional network structure of the carbon template. The mesopore surface area of the alumina can be as high as 365 $m^2 g^{-1}$, and the pore volume reaches 1.55 $cm^3 g^{-1}$ after calcination at 600 °C in air for 8 h. The pore parameters can be varied within a certain range by variation of the carbon aerogel template and the loading amount of the alumina precursor. At high loadings, the obtained glassy alumina clearly has a bimodal pore size distribution in the mesopore range.

Keywords: adsorption · carbon aerogel · mesoporous materials · nanocasting

Introduction

Porous aluminas are attractive materials with broad applicability as adsorbents, catalyst supports, and as part of bifunctional catalysts in large-scale processes in the chemical and petrochemical industry, such as the cracking and hydrocracking of petroleum, the purification of gas–oil fractions, or the steam reforming of hydrocarbon feedstocks to produce hydrogen. The wide range of applications of these aluminas can be traced back to their favorable textural properties, such as surface area, pore volume, and pore size distribution (PSD), as well as to their high thermal and hydrothermal stabilities. Due to the importance of alumina in catalysis, the ability to tailor its pore system is needed, and thus, several attempts have been made to synthesize mesoporous aluminas.[1–4] The discovery of the silica-based M41S family of mesoporous materials with a narrow pore size distribution has also promoted considerable activity in the development of ordered, mesoporous aluminas. Generally, all processes used in the surfactant-assisted synthesis of silicas are also employed in attempts to synthesize mesoporous aluminas, such as the routes that use neutral, anionic, cationic, or block-polymer surfactants. Pinnavaia et al. were the first to report the preparation of mesostructured wormhole-like alumina from aluminum tri-*sec*-butoxide in the presence of electrically neutral, block-copolymer surfactants as structure-directing agents.[5] Similar wormhole structures have also been synthesized by the hydrolysis of aluminum alkoxides assisted by the anionic surfactant sodium dodecylbenzenesulfonate[6] or the cationic surfactant cetyltrimethylammonium bromide.[7] Using the hydrolysis of alkoxides under basic conditions, Shanks and co-workers synthesized mesoporous alumina with a hierarchical structure, composed of mesopores 4 nm in diameter and macropores with a diameter of about 300 nm.[8] Lee et al. succeeded in synthesizing aluminas with unidirectional nanostructures, such as nanotubes, nanofibers, and nanorods, by the hydrolysis of aluminum alkoxides assisted by surfactants in the absence of a solvent.[9]

However, despite these successes, the synthesis of mesoporous alumina by surfactant-assisted methods poses more complex problems than the synthesis of analogous silica-based materials, because attempts to remove the surfactant often result in the structural collapse of the alumina mesopores. High degrees of structural order, which are common for silicas, are rarely observed for aluminas. Furthermore, the raw materials mostly used are expensive alkoxides, and the hydrolysis rate of such alkoxides is not easy to control. Yang et al. attempted to synthesize mesoporous alumina from aluminum nitrate by means of a sol–gel process assisted by ultrasound.[10] This reaction, however, is very sensitive to reaction conditions, which needed to be strictly controlled in order to form a gel precursor. The highest surface area

[a] Dr. W.-C. Li, Dr. A.-H. Lu, Dr. W. Schmidt, Prof. Dr. F. Schüth
Max-Planck-Institut für Kohlenforschung
Kaiser-Wilhelm-Platz 1, 45470 Mülheim (Germany)
Fax: (+49) 208-306-2995
E-mail: schueth@mpi-muelheim.mpg.de

DOI: 10.1002/chem.200400776

and pore volume achieved were 266 $m^2 g^{-1}$ and 0.2 $cm^3 g^{-1}$, respectively.

An alternative approach to structure alumina on the mesoscale is to use hard templates in a nanocasting process. There is one attempt reported in the literature to use a porous, ordered carbon of the CMK-3 type as a hard template to synthesize mesoporous alumina.[11] However, although a high surface area alumina was synthesized, the material was not highly ordered. The surface area and pore volume, on the other hand, were rather high, reaching 360 $m^2 g^{-1}$ and 0.36 $cm^3 g^{-1}$, respectively. In general, porous carbons are ideal exotemplate molds for the creation of high surface area materials and can easily be removed by simple combustion.[12] Wakayama and co-workers used activated carbons as templates; a metal-oxide precursor in a supercritical solvent was introduced by an impregnation process to synthesize nanoporous oxides.[13] A simpler approach is the direct impregnation of activated carbons with concentrated aqueous salt solution. After drying and removal of the carbon templates by combustion, porous metal oxides and even more complex oxides, such as spinels, with high surface areas can be achieved.[14,15] However, it is difficult to create porous metal oxides with controlled macroscopic morphologies and controllable pore size distributions by using activated carbons as templates. This is due to the limitations of activated carbons, which often have broad pore size distributions and are typically available in powder form or as formed bodies, which are generated from powders.

We therefore decided to investigate the use of carbon aerogels as hard templates for the synthesis of mesoporous alumina with a controllable pore size, high surface area, and high pore volume, by using aluminum nitrate as a cheap aluminum source. Such carbon aerogels are usually investigated for use as electrode materials of supercapacitors.[16,17] However, initial applications as hard templates are also emerging: carbon aerogel was recently used as a template to synthesize ZSM-5 monoliths with uniform mesoporous channels.[18] The templating function of carbon aerogels can be attributed to their unique properties, such as the three-dimensional connectivity of their pore system, high pore volume, and narrow pore size distribution. In addition, their purity is much higher than that of activated carbon. Because of their special nanostructure, carbon aerogels are ideal templates for exotemplate synthesis.[15] Herein we describe the synthesis of glassy alumina with exceptionally high pore volume by nanocasting from carbon aerogels, and the control of the alumina pore system by adjusting the properties of the aerogels.

Results and Discussion

The carbon aerogel was synthesized by using a sol–gel process, but drying could be carried out under ambient conditions after solvent exchange. Thus, supercritical drying, which is often used in the synthesis of high-porosity aerogels, could be avoided. Aluminum nitrate aqueous solution was infiltrated into the carbon aerogel by the incipient wetness technique, followed by simple drying and calcination. All of the experiments were carried out under ambient conditions. Therefore, this process is relatively simple compared to other synthesis routes for the preparation of high surface area/high pore volume alumina with an adjustable mesopore size.

Five carbon aerogels with different textural parameters were synthesized by varying the reaction conditions. Based on their increasing average pore size, the carbon aerogels obtained are denoted as CA-1, CA-2… in the tables and figures. The as-synthesized aluminas obtained from these gels are referred to as A-1, A-2, and so on, whereby the numbers refer to the carbon aerogel templates from which the alumina products were made. In addition, aluminas synthesized from CA-4 and CA-5 templates with higher amounts of alumina precursor are denoted as A-4-HA and A-5-HA, respectively. For synthesis details refer to the Experimental Section.

Morphology and structure: The aluminas obtained by using different Al_2O_3/C ratios were glassy in appearance and granular in shape (Figure 1). The as-synthesized alumina samples

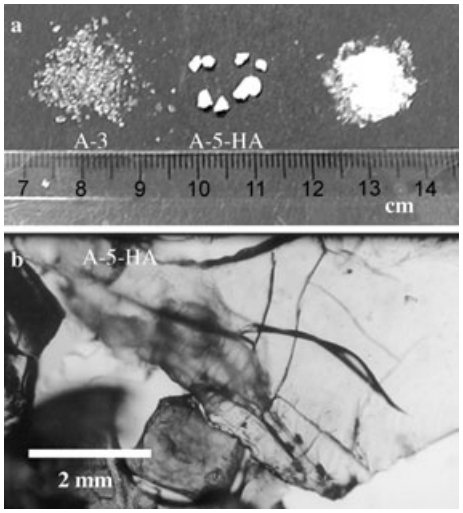

Figure 1. Optical photographs of as-synthesized glassy aluminas. a) Digital camera image of samples with low Al_2O_3/C ratio (left), high Al_2O_3/C ratio (middle), and alumina obtained when powdered porous carbon (CMK-3) was impregnated (right). b) Optical micrograph of a sample of the alumina material shown in the middle of (a), taken with a Leitz Orthoplan microscope.

obtained from composites (aluminum nitrate/dried carbon aerogel) with an Al_2O_3/C ratio below 0.2 were composed of small transparent granules 2–3 mm in diameter. A typical image of such an alumina (sample A-3) is given in Figure 1a (left). Such syntheses were repeated several times, confirming the reproducibility of the process. When the Al_2O_3/C ratio of the composite was higher than 0.3, the granules were larger with a diameter of 4–6 mm, as shown for sample A-5-HA in Figure 1a (middle). These bigger granules

appear white due to scattering losses. On a smaller scale, these samples are also glassy and transparent, as the micrograph in Figure 1b clearly shows. As a comparison, alumina was prepared by the same procedure, but with mesoporous carbon powder (CMK-3) as the template. The resulting alumina was a white powder (Figure 1a, right), quite different in appearance to the glassy samples obtained from the carbon aerogel template. This is due to the small particle size of the parent CMK-3, which leads to small-particle-sized alumina, in contrast to the millimeter-sized replicas from the aerogel, in which the absence of grain boundaries results in low light-scattering. The glassy, granular form of alumina is convenient for practical application in industrial processes unlike the powder form, which may possess drawbacks, such as dusting and high pressure-drops; such drawbacks cannot be fully prevented by shaping procedures.

The structures of these samples were characterized by X-ray diffraction (XRD) analysis. In all cases there were no discernable reflections observed, indicating that these aluminas are still amorphous, in spite of the 600 °C calcination temperature. For most precursors, various types of crystalline or partially crystalline transition aluminas are obtained at these temperatures.[19] Elemental analysis showed that the residue of carbon in the alumina was far below 0.5 wt % in all cases, indicating nearly complete removal of the carbon template at the calcination temperature used here. In the low-angle range, no Bragg peaks were detected, only a continuous decay of scattered intensity typical for high-surface-area materials. This indicates that a regular mesopore structure was not formed, the expected result for hard templating from a disordered carbon aerogel.

TEM analysis: The nanostructures of the carbon aerogel templates and the corresponding aluminas were characterized by TEM to ascertain the relationship between the textures of the templates and the products. Representative TEM images of carbon aerogels and the resulting aluminas are shown in Figure 2. The images of the carbon aerogels (CA-3 and CA-5) reveal their uniform structure, consisting of a well-defined three-dimensional network of spherical carbon particles. The estimated diameter of the spherical particles is around 10–15 nm. These primary particles are cross-linked with each other to form the abundant textural mesopores in the carbon aerogels.[20] Aluminas, with both low and high loading, formed by using such aerogels inherited the well-developed three-dimensional network structure of the parent carbon template, as shown in Figure 2 (A-3 and A-5-HA). This is evidence of the replication of the network structure of the carbon aerogel; that is, the resulting alumina preserves the nanostructure of the carbon template well. Also, the fact that millimeter-sized granules (Figure 1) were obtained demonstrates the preservation of the 3D pore connectivity in the resulting alumina. In particular, the higher alumina loading (Al_2O_3/C ratio >0.3) resulted in larger sized granules of alumina, as seen in Figure 1, which can be attributed to improved pore filling resulting in the formation of a more fully connected, rigid framework. After removal of the carbon template, this rigid framework is best at copying the nanostructure of the carbon aerogel. However, differing from the spherically shaped, primary carbon particles of the aerogel, the primary alumina particles exhibited a more sausage-like morphology. This is understandable because the alumina should reflect the morphology of the pore structure. The diameter of the alumina particles was estimated to be 5–7 nm. An increased amount of alumina precursor did not seem to change the overall morphology of the resulting alumina particles, but instead increased the particle diameters (Figure 2).

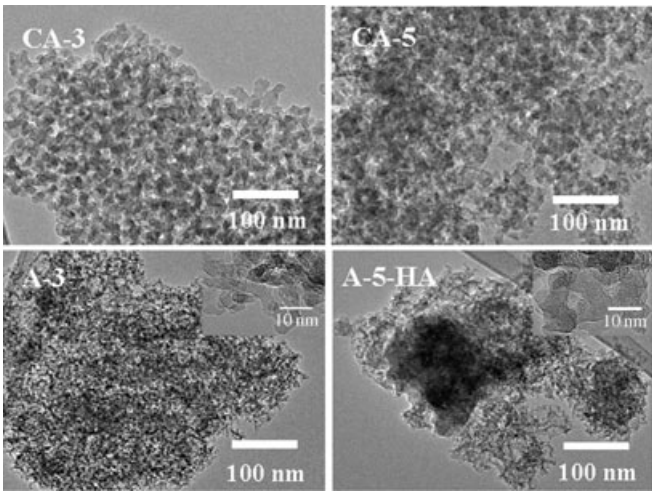

Figure 2. TEM images of carbon aerogel templates (CA-3 and CA-5) and the corresponding mesoporous aluminas (A-3 and A-5-HA).

Sorption analysis: To further substantiate the templating effect and to obtain more information on the pore structure of the carbon aerogel and the alumina, the materials were investigated by nitrogen sorption measurements. The nitrogen sorption isotherms for the carbon aerogel templates and the corresponding aluminas synthesized at low loadings are displayed in Figure 3. The template textural parameters, such as the surface area, total pore volume, and pore size, are compiled in Table 1. The carbon aerogel templates have a type IV isotherm with well-pronounced H1 type hysteresis loops in the relative pressure range of 0.7–0.9 (Figure 3a). At relative pressures below 0.1, the high uptake of nitrogen indicates the presence of micropores in the carbon aerogels, in agreement with the micropore volume determined by means of the *t*-plot method. The nitrogen sorption isotherms for the aluminas (Figure 3b) are also of type IV with a significant amount of nitrogen adsorbed at relative pressures close to unity. More surprisingly, a very high pore volume of $1.55\ cm^3 g^{-1}$ was achieved for alumina A-5 (Table 2). As seen from Figure 3b, the amount of nitrogen adsorbed at low pressure is negligible, and the micropore volumes calculated from the *t*-plot method (Table 2) are extremely low relative to those of the carbon templates. In addition, the mesopore surface area of the alumina estimated by the *t*-plot method (Table 2) is essentially equal to the total Brun-

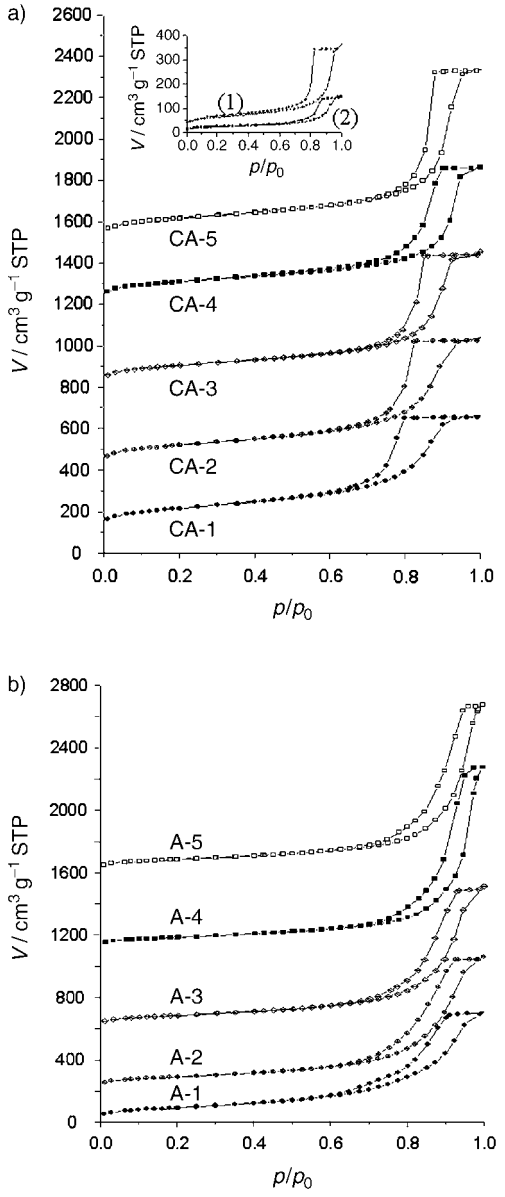

Figure 3. Nitrogen sorption isotherms of a) carbon aerogels and b) the corresponding mesoporous aluminas synthesized at low Al_2O_3/C ratios. The isotherms of CA-2, CA-3, CA-4, and CA-5 were offset vertically by 300, 700, 1100, and 1400 $cm^3 g^{-1}$ STP, respectively. The isotherms of A-2, A-3, A-4, and A-5 were offset vertically by 200, 600, 1100, and 1600 $cm^3 g^{-1}$ STP, respectively. The inset isotherms in a) are those of dried carbon aerogel/aluminum nitrate composite-1 and composite-2 (see footnotes of Table 2), with Al_2O_3/C ratios of 0.16 and 0.34, respectively.

auer–Emmet–Teller (BET) surface area. This indicates that the porosity of the alumina can mainly be attributed to the mesopores. The adsorption branches of the isotherms of alumina A-4 and A-5, synthesized at-low-precursor-loading levels, do not clearly reach a plateau at high relative pressure, indicating the existence of larger macropores, which cannot be detected by the nitrogen adsorption technique.

The pore size distributions (PSDs) for the carbon aerogel templates calculated from the desorption branch, by means of the Barrett–Joyner–Halenda (BJH) model, are quite narrow and centered around 10–14 nm (Figure 4a). In contrast, the aluminas display relatively broad PSDs in the range of 5–30 nm (Figure 4b). The ratio of alumina to carbon (Al_2O_3/C) was below 0.2 for these samples. Such low impregnated amounts are not sufficient to sustain the skeleton architecture of the carbon aerogel templates after removal of the carbon. Partial collapse of the pore structures would result in an aggregation of alumina particles, finally leading to the formation of large pores and a broad pore size distribution due to the statistical nature of the process. However, it should be mentioned that with an increasing average pore size of the carbon templates from 8.1 to 13.6 nm (CA-1 to CA-5, Table 1), the average pore size of the corresponding aluminas (A-1 to A-5) increased as well from 10.4 to 16.6 nm (Table 2). A clear one-to-one correspondence between the pore sizes of the carbon aerogel and the alumina cannot be expected, as the pores in the alumina should correspond to the particles of the aerogel. However, coarsening of the pore structure in a gel such as the carbon aerogel generally corresponds to a coarsening of the particulate structure of the gel.[21] Therefore, one would expect the textural trends to be identical for "mold" and "cast", as is in fact observed experimentally. Hence, we can deduce that the alumina mesopore structure, at least to some extent, reflects the network structure of the carbon aerogel template.

When the Al_2O_3/C ratio was higher than 0.3, the aluminas obtained unexpectedly showed a double hysteresis loop in the relative pressure ranges of 0.7–0.9 and 0.9–1.0 (Figure 5). This demonstrates the existence of a bimodal pore system in samples A-4-HA and A-5-HA, as further verified by the PSDs of these aluminas (Figure 5, inset). These PSDs clearly show two maxima at 8 nm and around 20–30 nm. We suggest that the small mesopores are generated from the spaces in which the carbon aerogel primary particles were positioned, and the larger mesopores result from the aggregation of the alumina primary particles.

As stated above, the alumina precursor was introduced in the form of an aqueous solution of aluminum nitrate. Evidently, it was impossible to completely fill the pore system of the carbon aerogel with alumina by single-step impregnation, because part of the pore space of the carbon aerogel was still accessible after water removal. To achieve higher loadings of alumina the impregnation procedure needs to be repeated. However, if one analyses the isotherms (Figure 3a, inset) and textural parameters (Table 2) of Al_2O_3/C composites-1 and -2 before carbon removal, the shape of both the isotherms is similar for high and low alumina loadings, if one disregards the decreases in surface area and pore volume. This seems to suggest that there are parts of the pore system completely filled, and that other parts are still more or less empty. After repeated impregnation, the surface area and pore volume were strongly reduced: the values for composite-2, with a high alumina loading, were 0.22 $cm^3 g^{-1}$ and 87 $m^2 g^{-1}$, respectively. Thus, nearly complete filling of the carbon aerogel pore space (i.e., 70%) could be achieved. It is reasonable to infer that at higher

Table 1. Synthesis conditions and textural parameters of carbon aerogels.

Sample	C_{syn}[a]	Catalyst	S_{BET}[b] [$m^2 g^{-1}$]	S_{meso}[b] [$m^2 g^{-1}$]	V_{total}[b] [$cm^3 g^{-1}$]	V_{mic}[b] [$cm^3 g^{-1}$]	D_{BJH}[b] [nm]
CA-1	30/200	$Ca(OH)_2$	740	367	1.0	0.16	8.1
CA-2	40/200	$Ca(OH)_2$	747	344	1.12	0.17	9.6
CA-3	30/500	Na_2CO_3	697	299	1.14	0.17	11.5
CA-4	40/500	Na_2CO_3	709	296	1.17	0.17	11.6
CA-5	40/500	Na_2CO_3[c]	752	329	1.44	0.17	13.6

[a] C_{syn}: synthesis conditions of carbon aerogels. For example, 30/200 means the percentage of resorcinol and formaldehyde was 30 wt%, and the molar ratio of resorcinol/catalyst was 200, and so on. [b] S_{BET}: specific surface area calculated based on the BET theory; S_{meso} and V_{mic}: mesopore surface area and micropore volume calculated with the *t*-plot method; V_{total}: single-point total pore volume; D_{BJH}: average pore diameter calculated with the BJH method (desorption branch). [c] For the CA-5 catalyst specifically, Na_2CO_3 was dissolved in a saturated aqueous solution of magnesium hydroxide, in which the Mg^{2+} ion concentration was determined to be 0.0018 M.

Table 2. Textural parameters of composites and mesoporous aluminas.[a]

Sample	S_{BET} [$m^2 g^{-1}$]	S_{meso} [$m^2 g^{-1}$]	V_{total} [$cm^3 g^{-1}$]	V_{mic} [$cm^3 g^{-1}$]	D_{BJH} [nm]	Al_2O_3/C
composite-1[b]	224	133	–	0.03	10.5	0.16
composite-2[c]	87	19	0.22	0.01	12.1	0.34
A-1	335	339	1.07	0.02	10.4	0.09
A-2	332	365	1.30	0.01	12.2	0.14
A-3	311	309	1.41	0.01	14.0	0.16
A-4	305	267	1.55	0.01	17.9	0.19
A-5	300	281	1.48	0.01	16.6	0.18
A-4-HA	278	261	1.03	0.01	7.7, 22.9[d]	0.34
A-5-HA	275	256	0.80	0.01	7.7, 21.2[d]	0.34

[a] See Table 1 for parameter definitions. [b] Composite-1 is dried CA-3 carbon aerogel/aluminum nitrate, which resulted in the formation of A-3. [c] Composite-2 is dried CA-4 carbon aerogel/aluminum nitrate, which resulted in the formation of A-4-HA. [d] Maxima of the two peaks in the pore size distribution.

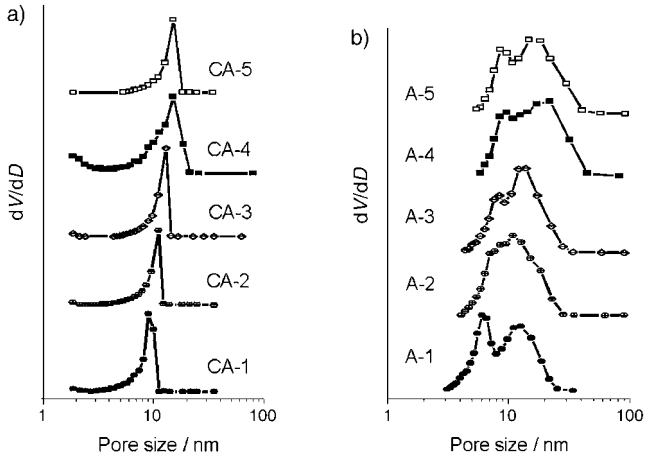

Figure 4. PSDs of a) carbon aerogels and b) the corresponding mesoporous aluminas synthesized at low Al_2O_3/C ratios.

filling levels the alumina primary particles are bigger and better connected, forming a strong, three-dimensional network. Removal of the carbon primary particles generates the voids in the alumina. From TEM observations (Figure 2), the primary particles of the carbon aerogel were around 10–15 nm in diameter. The pore size of the resulting alumina was smaller, at about 8 nm (Table 2 and PSDs in Figure 5, inset). This can be attributed to the thermal shrinkage of the structure during carbon removal. Only 70% of the pore space of the carbon aerogel was filled by the alumina precursor even at high loading levels. This means that some additional void space is formed during the process. This could occur homogeneously over the whole sample, by which a monomodal pore system would be formed. Alternatively, alumina may aggregate in domains of the sample, truly replicating the carbon, while, in between these domains larger pores would form. This would result in a bimodal pore size distribution, as observed in our samples (for instance, inset in Figure 5). We thus suggest that the second mechanism is valid for our materials. Such a hierachical combination of smaller and larger mesopores would actually be favorable from an application point of view, as this would, for example, reduce transport limitations in heterogeneous catalysis.[22–24]

As mentioned earlier and shown in Figure 1a, alumina synthesized by using powdered mesoporous carbon (CMK-3), with a 3.5 nm pore size, as the template, but otherwise by means of the same synthesis strategy, was obtained as a white powder with a surface area of only 177 $m^2 g^{-1}$ and a pore volume of 0.35 $cm^3 g^{-1}$; these values were much lower than that of the carbon-aerogel-

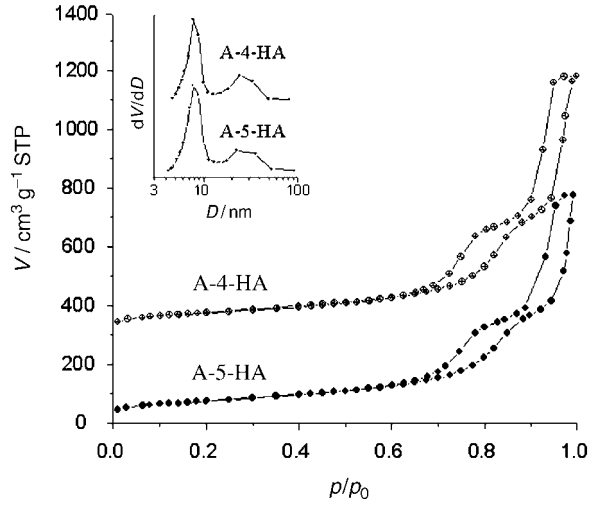

Figure 5. Nitrogen sorption isotherms and PSDs (inset) of aluminas synthesized with a high Al_2O_3/C ratio. The isotherms of A-4-HA are offset vertically by 300 $cm^3 g^{-1}$ STP.

templated alumina. From this observation we can conclude that carbon aerogel is the essential factor in forming the glassy alumina with a high pore volume.

Thermal behavior: As discussed above, the as-prepared aluminas with large pore volumes and high surface areas were amorphous after heat treatment at 600 °C in air for 8 h. In many cases the thermal stability of mesoporous alumina is particularly important due to the existence of many phases. Therefore, we also studied the thermal behavior of the aluminas discussed here at higher temperatures, by using sample A-4-HA as an example. Four derivatives were obtained through calcination of A-4-HA at either 700, 800, 900, or 1000 °C in air for 1 h. The obtained products still possessed the glassy, granular appearance. XRD analysis (Figure 6) of the sample calcined at 700 °C showed no clear

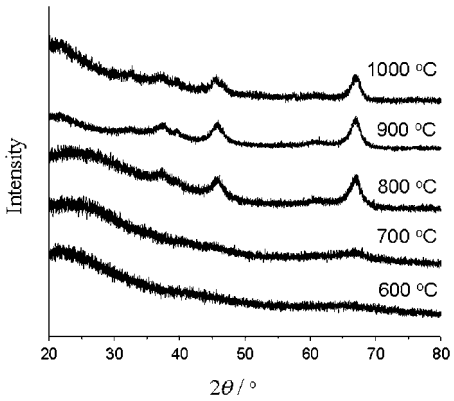

Figure 6. XRD patterns of mesoporous aluminas calcined in air at different temperatures.

reflections, confirming that the sample was still amorphous. After calcination at 800 °C and above, the samples showed broad, but clearly discernible, XRD reflections, indicating formation of a crystalline phase, which was identified as γ-alumina (JCPDS card 10–425). Nitrogen adsorption isotherms of the annealed samples have similar shapes to that of the parent alumina A-4-HA, that is, with two distinct capillary condensation steps, as shown in Figure 7. The calculated textural parameters (Table 3), however, indicate that both the surface area and pore volume gradually decrease at higher calcination temperature. Nevertheless, even at 1000 °C, the samples retained a high pore volume of around 0.4 $m^3 g^{-1}$ and a surface area of around 110 $m^2 g^{-1}$. Due to sintering, the pore diameters increased from 14.5 to 19.6 nm upon increasing the calcination temperature from 600 to 1000 °C.

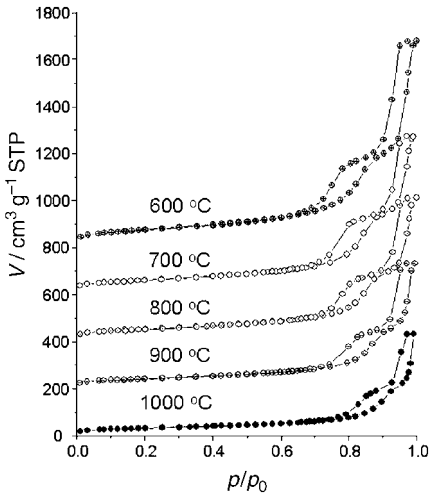

Figure 7. Nitrogen sorption isotherms of the A-4-HA aluminas calcined at 600, 700, 800, 900, and 1000 °C. The isotherms of the samples at calcination temperatures 900, 800, 700, and 600 °C were offset vertically by 200, 400, 600, and 800 $cm^3 g^{-1}$ STP, respectively.

Table 3. Textural parameters of mesoporous aluminas calcined at different temperatures.[a]

Temperature [°C]	S_{BET} [$m^2 g^{-1}$]	S_{meso} [$m^2 g^{-1}$]	V_{total} [$cm^3 g^{-1}$]	V_{mic} [$cm^3 g^{-1}$]	D_{BJH} [nm]
600	278	261	1.03	0.01	14.5
700	209	200	0.84	–	14.2
800	180	176	0.71	–	15.8
900	151	140	0.50	–	15.8
1000	112	100	0.38	–	19.6

[a] See Table 1 for parameter definitions.

Conclusion

In conclusion, a glassy, amorphous, mesoporous alumina with very high pore volume, high surface area, and controllable pore size has been synthesized by a simple impregnation and calcination method, with a carbon aerogel template and an aluminum nitrate solution as the alumina precursor. The alumina generated exhibits high mesopore surface area of up to 365 $m^2 g^{-1}$ and high pore volumes of up to 1.55 $cm^3 g^{-1}$. The pore parameters can be tuned within a certain range through variation of the pore size of the carbon aerogel template and the loading of the pore system with the alumina precursor. The glassy, granular aluminas may be useful for various applications, such as for supports in heterogeneous catalysis, as they can be handled easily and cleanly, and have very interesting textural, thermal, and structural properties. The synthesis strategy described might open a new route to fabricate mesoporous aluminas with a strongly interconnected pore system. Moreover, one can probably use porous carbon aerogels as the template for many different oxide products, as long as their precursors can be introduced into a porous carbon and retain the framework during carbon combustion.

Experimental Section

Synthesis of carbon aerogel templates: Carbon aerogels were based on resorcinol–formaldehyde polymers. The typical procedure to synthesize a

carbon aerogel was as follows: resorcinol (4 g; Fluka 99%) and formaldehyde (5.9 g; Fluka 36.5% in water, methanol-stabilized) were dissolved in deionized water (5.6 mL), and then sodium carbonate (0.0077 g; Fluka 99.5%) was added to the solution as polymerization catalyst, unless otherwise stated (Table 1). A homogeneous solution was prepared under magnetic stirring. The solutions obtained were cast into glass ampoules and were all cured by using the same procedure: one day at room temperature, one day at 50°C, and three days at 90°C. After the curing steps, the wet gels were introduced into acetone to exchange the water inside the pores and then dried under ambient pressure and room temperature to obtain the corresponding aerogels. The resulting aerogels were pyrolyzed at temperatures of up to 800°C in an argon atmosphere and thus transformed into monolithic carbon aerogels. During this study the R/F (resorcinol/formaldehyde) molar ratio was fixed at 0.5. The percentage of resorcinol and formaldehyde and the R/C (resorcinol/catalyst) molar ratio were varied in the range of 30–40 wt% and 200–500 (see Table 1), respectively, to obtain carbon aerogels with different pore sizes. The detailed synthesis conditions for each sample are listed in Table 1.

Synthesis of mesoporous aluminas: Aluminum nitrate (Fluka 98%) dissolved in deionized water at a concentration of 2.43 M was used as the alumina precursor. The solution was introduced into the carbon aerogels by incipient wetness impregnation at room temperature followed by a drying step at 50°C for several hours. Subsequently, a second impregnation could be carried out, and generally the impregnation and drying procedure was repeated two to three times to reach a high loading. Glassy alumina with a granular size of several millimeters was achieved by calcination of the dried aluminum nitrate/carbon composite at 600°C for 8 h in a muffle oven.

Characterization: Optical photographs were recorded either with a standard digital camera or a Leitz Orthoplan microscope. High-resolution TEM characterization was performed with a Hitachi HF2000 microscope equipped with a cold field emission gun. The acceleration voltage was 200 kV. Samples for TEM analysis were prepared dry on a fine carbon grid. X-ray diffraction patterns of the samples were recorded with a Stoe STADI P diffractometer in the Bragg–Brentano (reflection) geometry. Nitrogen adsorption isotherms were measured with an ASAP2010 adsorption analyzer (Micromeritics) at 77 K. Before the sorption measurements, all the samples were degassed at a temperature of 250°C for at least 6 h. Pore sizes and pore size distributions were calculated by the BJH method from the desorption branch. Total pore volume was estimated from the amount adsorbed at $p/p_0 = 0.99$. Specific surface areas were determined by the BET method and mesopore surface areas were calculated by the *t*-plot method.

Acknowledgements

We are grateful to Mr. Spliethoff for carrying out TEM measurements. A.-H.L. would like to thank the Alexander von Humboldt Foundation for a fellowship. Additional funding was received from the DFG through the Leibniz-Program, which is gratefully acknowledged.

[1] X. Liu, Y. Wei, D. Jin, W. Shih, *Mater. Lett.* **2000**, *42*, 143.
[2] S. Valange, J. L. Guth, F. Kolenda, S. Lacombe, Z. Gabelica, *Microporous Mesoporous Mater.* **2000**, *35*, 597.
[3] Z. Zhang, T. J. Pinnavaia, *J. Am. Chem. Soc.* **2002**, *124*, 12294.
[4] L. Sicard, B. Lebeau, J. Patarin, F. Kolenda, *Stud. Surf. Sci. Catal.* **2002**, *143*, 209.
[5] S. A. Bagshaw, T. J. Pinnavaia, *Angew. Chem.* **1996**, *108*, 1180; *Angew. Chem. Int. Ed. Engl.* **1996**, *35*, 1102.
[6] F. Vaudry, S. Khodabandeh, M. E. Davis, *Chem. Mater.* **1996**, *8*, 1451.
[7] S. Cabrera, J. E. Haskouri, J. Alamo, A. Beltrán, D. Beltrán, S. Mendioroz, M. D. Marcos, P. Amorós, *Adv. Mater.* **1999**, *11*, 379.
[8] W. Deng, M. W. Toepke, B. H. Shanks, *Adv. Funct. Mater.* **2003**, *13*, 61.
[9] H. C. Lee, H. J. Kim, S. H. Chung, K. H. Lee, H. C. Lee, J. S. Lee, *J. Am. Chem. Soc.* **2003**, *125*, 2882.
[10] N. Yao, G. Xiong, Y. Zhang, M. He, W. Yang, *Catal. Today* **2001**, *68*, 97.
[11] F. Schüth, T. Czuryskiewicz, F. Kleitz, M. Linden, A.-H. Lu, J. Rosenholm, W. Schmidt, A. Taguchi, *Stud. Surf. Sci. Catal.* **2003**, *146*, 399.
[12] F. Schüth, W. Schmidt, *Adv. Mater.* **2002**, *14*, 629.
[13] H. Wakayama, S. Inagaki, Y. Fukushima, *J. Am. Ceram. Soc.* **2002**, *85*, 161.
[14] M. Schwickardi, T. Johann, W. Schmidt, F. Schüth, *Chem. Mater.* **2002**, *14*, 3913.
[15] F. Schüth, *Angew. Chem.* **2003**, *115*, 3730; *Angew. Chem. Int. Ed.* **2003**, *42*, 3604.
[16] A. C. Pierre, G. M. Pajonk, *Chem. Rev.* **2002**, *102*, 4243.
[17] W. Li, G. Reichenauer, J. Fricke, *Carbon* **2002**, *40*, 2955.
[18] Y. Tao, H. Kanoh, K. Kaneko, *J. Am. Chem. Soc.* **2003**, *125*, 6044.
[19] P. Euzen, P. Raybaud, X. Krokidis, H. Toulhoat, J. L. Loarer, J. P. Jolivet, C. Froidefond, *Handbook of Porous Solids, Vol. 3*, (Eds.: F. Schüth, K. S. W. Sing, J. Weitkamp), Wiley-VCH, Weinheim, **2002**, p. 1591.
[20] S. A. Al-Muhtaseb, J. A. Ritter, *Adv. Mater.* **2003**, *15*, 101.
[21] V. Bock, A. Emmerling, J. Fricke, *J. Non-Cryst. Solids* **1998**, *225*, 69.
[22] D. R. Rolison, *Science* **2003**, *299*, 1698.
[23] S. T. Wong, H. P. Lin, C. Y. Mou, *Appl. Catal. A* **2000**, *198*, 103.
[24] L. Z. Zhang, J. C. Yu, *Chem. Commun.* **2003**, 2078.

Received: July 29, 2004
Revised: November 12, 2004
Published online: January 24, 2005